EFDA–JET–PR(14)18

C. Hellesen, J. Eriksson, F. Binda, S. Conroy, G. Ericsson, A. Hjalmarsson,
M. Skiba, M. Weiszog and JET EFDA contributors

Fuel Ion Ratio Measurements in NBI Heated Deuterium Tritium Fusion Plasmas at JET using Neutron Emission Spectrometry

Fuel Ion Ratio Measurements in NBI Heated Deuterium Tritium Fusion Plasmas at JET using Neutron Emission Spectrometry

C. Hellesen[1], J. Eriksson[1], F. Binda[1], S. Conroy[1], G. Ericsson[1], A. Hjalmarsson[1], M. Skiba[1], M. Weiszog[1] and JET EFDA contributors*

JET-EFDA, Culham Science Centre, OX14 3DB, Abingdon, UK

[1]EURATOM-VR, Deptartment of Physics and Astronomy, Uppsala University, Sweden
** See annex of F. Romanelli et al, "Overview of JET Results", (24th IAEA Fusion Energy Conference, San Diego, USA (2012)).*

Preprint of Paper to be submitted for publication in
Nuclear Fusion

ABSTRACT

The fuel ion ratio ($n_{\rm t}/n_{\rm d}$) is of central importance for the performance and control of a future burning fusion plasma, and reliable measurements of this quantity are essential for ITER. This paper demonstrates a method to measure the core fuel ion ratio by comparing the thermonuclear and beam-thermal neutron emission intensities, using a high resolution neutron spectrometer. The method is applied to NBI heated deuterium tritium (DT) plasmas at JET, using data from the magnetic proton recoil (MPR) spectrometer. The trend in the results is consistent with Penning trap measurements of the fuel ion ratio at the edge of the plasma, but there is a discrepancy in the absolute values, possibly owing to the fact that the two measurements are weighted towards different parts of the plasma. It is suggested to further validate this method by comparing it to the traditionally proposed method to estimate $n_{\rm t}/n_{\rm d}$ from the ratio of the thermal DD and DT neutron emission components. The spectrometer requirements for measuring $n_{\rm t}/n_{\rm d}$ at ITER are also briefly discussed.

1. INTRODUCTION

In a fusion plasma fueled with deuterium (D) and tritium (T) the neutron emissivity is given by $R_{\rm dt} = n_{\rm d} n_{\rm t} \langle \sigma v \rangle_{\rm dt}$, where $n_{\rm d}$ is the deuterium density, $n_{\rm t}$ is the tritium density and $\langle \sigma v \rangle_{\rm dt}$ is the DT reactivity. The optimum fuel ion mix is an equal mixture of D and T, i.e. a fuel ion ratio $n_{\rm t}/n_{\rm d} = 1.0$. Changes in the fusion power could be either due to variations in the plasma core density, the core ion temperature ($T_{\rm i}$) and hence the reactivity, the core fuel ion ratio, or combinations thereof. For efficient burn control of a plasma it is therefore important to be able to measure all these parameters of the fuel ions.

This paper presents measurements of the neutron emission spectrum from which we estimate the core fuel ion ratio in ITER relevant plasma conditions at JET. The data were taken during the JET DTE1 experiment in 1997. Existing methods that were used to measure $n_{\rm t}/n_{\rm d}$ during the JET DT program were low energy neutral particle analyzers (NPA) as well as a Penning trap that analyzed neutral gases collected below the divertor. However, none of these methods measured the fuel ion ratio in the core plasma.

Apart from neutron spectrometry, it has been proposed to measure the core fuel ion ratio using e.g. charge exchange recombination spectroscopy (CXRS) and collective Thomson scattering [1]. One benefit of neutron-based measurements is that they are typically not hampered by high neutron rates, which can be a problem for other diagnostic techniques [2]. In fact, neutron measurements benefit from high rates in the sense that the statistics are improved.

It has been suggested [3, 4] to obtain $n_{\rm t}/n_{\rm d}$ from the ratio of the 14 MeV DT and the 2.5 MeV DD emission rates, $R_{\rm dt}$ and $R_{\rm dd}$, respectively. The DD rate is given by $R_{\rm dd} = n_{\rm d}^2 \langle \sigma v_{\rm rel} \rangle_{\rm dd} /2$, and

the fuel ion ratio is then given by

$$\frac{n_{\mathrm{t}}}{n_{\mathrm{d}}} = \frac{R_{\mathrm{dt}} \left\langle \sigma v_{\mathrm{rel}} \right\rangle_{\mathrm{dd}}}{2R_{\mathrm{dd}} \left\langle \sigma v_{\mathrm{rel}} \right\rangle_{\mathrm{dt}}}. \tag{1}$$

There are, however, two things that complicate this measurement.

First, supra thermal components in the neutron emission, mainly from plasma heating with neutral beam injection (NBI), will interfere with the thermonuclear emission. If high-resolution neutron spectrometers are not used to resolve the thermonuclear contribution from the supra thermal, the method of comparing R_{dt} and R_{dd} is limited to purely thermonuclear plasmas, i.e., ohmic plasmas or some scenarios relying exclusively on minority ion cyclotron radio frequency (ICRF) heating.

Second, energy degraded scattered neutrons from the DT emission will show up as a continuous tail below the 14 MeV peak, extending down to zero energy. If the ratio of DT to DD emission is too high, the DD signal will not be distinguishable from the background of scattered DT neutrons. In fact, this occurs already around $R_{\mathrm{dt}}/R_{\mathrm{dd}} = 70$, which corresponds to $n_{\mathrm{t}}/n_{\mathrm{d}} > 0.1 - 0.2$, depending on the measurement conditions [4]. Consequently, the most important region in the fuel ion ratio, i.e., $n_{\mathrm{t}}/n_{\mathrm{d}} = 1.0$, cannot be covered using this technique. However, we can exploit the information on the fuel ions that is carried by the supra thermal emission from the NBI heating. The fuel ion ratio can then be estimated by analyzing the DT emission alone. Since the DD emission is not used, scattered neutrons will not hamper the measurements, and the region around $n_{\mathrm{t}}/n_{\mathrm{d}} = 1.0$ can be covered.

In this paper we analyze DT plasmas from the DTE1 campaign at JET in 1997, and data from the MPR spectrometer [5] are used to obtain estimates of $n_{\mathrm{t}}/n_{\mathrm{d}}$. In section 2 it is described how the fuel ion ratio can be estimated from measurements of thermal and supra-thermal neutron emission intensities. Section 3 describes the MPR neutron spectrometer and the JET discharges that were studied in the present analysis. Estimated fuel ion ratios for these JET discharges are presented in section 4. The results are discussed in section 5, along with a short outlook about future work at JET and the implications for fuel ion ratio measurements at ITER. Finally, the conclusions of the study are presented in section 6.

2. INFORMATION IN THE NEUTRON EMISSION

In a NBI heated plasma there are a number of possible contributions to the neutron production: thermonuclear (TH), beam-thermal (NB) and beam-beam (BB) from DD, DT, TD[1] and TT reactions. However, for high plasma densities and fuel ion ratios around one (i.e., relevant for burning plasmas) the thermonuclear DT emission, together with beam-thermal emission where applicable, will completely dominate. Because of this we will omit all other reactions in this paper, although they will contribute to the neutron emission, but not at a significant level. In a fusion reaction

[1] The terminology TD is here used to denote reactions from a T-beam interacting with a thermal D-plasma.

between two ion species, *i* and *j*, the directional reactivity is given by

$$r_{ij}\left(\mathbf{x},\mathbf{u}\right)=\frac{1}{1+\delta_{ij}}\int\int f_i\left(\mathbf{v}_i,\mathbf{x}\right)f_j\left(\mathbf{v}_j,\mathbf{x}\right)\sigma\left(v_{\mathrm{rel}},\mathbf{u}\right)v_{\mathrm{rel}}\,\mathrm{d}\mathbf{v}_i\,\mathrm{d}\mathbf{v}_j. \tag{2}$$

Here $\mathbf{x}$ is the position in the plasma, and $\mathbf{u}$ is the direction of the neutron emission. f_i and f_j are the distribution functions of the two ion species, and $\sigma\left(v_{\mathrm{rel}},\mathbf{u}\right)$ is the cross section of the reaction. Since a neutron spectrometer measures a collimated flux, the emissivity needs to be integrated along the spectrometer sight line. The fluxes from thermonuclear reactions ($I_{\mathrm{TH,DT}}$), beam-thermal DT reactions ($I_{\mathrm{NB,DT}}$) and beam-thermal TD reactions ($I_{\mathrm{NB,TD}}$) can be approximated by

$$I_{\mathrm{TH,DT}}\approx\frac{n_{\mathrm{d}}}{n_{\mathrm{e}}}\frac{n_{\mathrm{t}}}{n_{\mathrm{e}}}\int n_{\mathrm{e}}^2\left(\mathbf{x}\right)r_{\mathrm{th,th}}\Omega\left(\mathbf{x}\right)\,\mathrm{d}\mathbf{x} \tag{3}$$

$$I_{\mathrm{NB,DT}}\approx\frac{n_{\mathrm{t}}}{n_{\mathrm{e}}}\int n_{\mathrm{nb,d}}\left(\mathbf{x}\right)n_{\mathrm{e}}\left(\mathbf{x}\right)r_{\mathrm{nb,th}}\Omega\left(\mathbf{x}\right)\,\mathrm{d}\mathbf{x} \tag{4}$$

$$I_{\mathrm{NB,TD}}\approx\frac{n_{\mathrm{d}}}{n_{\mathrm{e}}}\int n_{\mathrm{nb,t}}\left(\mathbf{x}\right)n_{\mathrm{e}}\left(\mathbf{x}\right)r_{\mathrm{nb,th}}\Omega\left(\mathbf{x}\right)\,\mathrm{d}\mathbf{x} \tag{5}$$

where $\Omega\left(\mathbf{x}\right)$ is the solid angle covered by the spectrometer at position $\mathbf{x}$. To obtain the corresponding total neutron rates, in this paper referred to as $R_{\mathrm{TH,DT}}$, $R_{\mathrm{NB,DT}}$, $R_{\mathrm{NB,TD}}$ and R_{NT} for their sum, the integrals are instead calculated over the entire plasma volume and the solid angle coverage is set to $\Omega=4\pi$. An approximation is used here where the relative fuel ion densities, $n_{\mathrm{d}}/n_{\mathrm{e}}$ and $n_{\mathrm{t}}/n_{\mathrm{e}}$, are lifted out of the integrals in equations (3)-(5). The assumption that has to be made is that the profiles of Z_{eff} and $n_{\mathrm{t}}/n_{\mathrm{d}}$ are constant in the core plasma, where the significant neutron production occurs. The integrals are instead calculated using the electron density profile, $n_{\mathrm{e}}\left(\mathbf{x}\right)$. The benefit of doing so is that one only needs to perform the calculations once for each plasma condition. The relative fuel ion densities, and thereby $n_{\mathrm{t}}/n_{\mathrm{d}}$, can then be deduced from measurements of R_{NT} and $I_{\mathrm{TH}}/I_{\mathrm{NB}}$.

Note that the use of the double differential cross section, $\sigma=\sigma\left(v_{\mathrm{rel}},\mathbf{u}\right)$, is required if either of the velocity distributions is anisotropic. This applies to supra-thermal distributions from auxiliary heating. When calculating the total neutron rates, or if both distributions are isotropic, as is the case with thermonuclear reactions, it suffices to use the single differential cross section $\sigma=\sigma\left(v_{\mathrm{rel}}\right)$.

In this paper we solve the integrals (3) through (5) using the Monte Carlo code ControlRoom. An early version of this code was used in [6]. In ControlRoom the velocity $\mathbf{v}$ is sampled for the thermal and beam slowing-down distributions, and the location $\mathbf{x}$ is sampled in the spectrometer sight line, which is presented in section 3 of this paper. Each sampled position in the sight line has a local direction of emission $\mathbf{u}\left(\mathbf{x}\right)$ and solid angle coverage $\Omega\left(\mathbf{x}\right)$. A distribution in thermal equilibrium is given by $f_{\mathrm{th}}\left(\mathbf{v}\right)=\exp\left(-m\mathbf{v}^2/2k_{\mathrm{b}}T\right)$, and one only needs the temperature at $\mathbf{x}$ to fully specify f_{th}. On the other hand, the slowing down distribution from NBI heating, f_{nb}, needs to be calculated numerically. In this paper we use the code NUBEAM [7], which is a part of the TRANSP package [8] and provides f_{nb} in 4 dimensions: R, Z, E and $v_{\parallel}/v$. The energy spectrum of the flux $\mathrm{d}n/\mathrm{d}E$ can also be calculated if the resulting neutron energy from each pair of sampled velocities v_i and v_j is calculated and a histogram with the appropriate weights is made [9].

3. EXPERIMENTAL

3.1. THE MPR SPECTROMETER

The neutron spectral measurements presented in this paper are made with the magnetic proton recoil (MPR) spectrometer [5]. In the MPR, a collimated neutron beam from the plasma impinges a thin plastic foil, producing recoil protons through elastic n-p scattering. A collimation of the recoil protons singles out the head on collisions, which gives $E_{\mathrm{p}} \approx E_{\mathrm{n}}$. The protons are subsequently momentum analyzed in a magnetic system, and their energy spectrum is obtained as a position histogram on a 520 mm wide hodoscope consisting of 36 scintillator detectors. The width of the hodoscope is equivalent to an energy bite of about 11.5 MeV to 17 MeV, and the mapping of neutron energies to hodoscope position is near-Gaussian. The spectrometer settings used together with the corresponding energy resolution and efficiency are given in table 1.

The MPR spectrometer is installed at JET with a quasi-tangential sight line that makes a double pass through the plasma center. In figure 1 the position dependent solid angle covered by the spectrometer, $\Omega(\mathbf{x})$, is shown projected on the RZ and XY planes. For the RZ projection, the direction towards the spectrometer, $\mathbf{u}$, is also shown to illustrate the curvature of the sight line in this projection. The sight line was calculated with the code LINE-21 [10].

3.2. JET DISCHARGES STUDIED

Four discharges, with properties suited for the analysis presented here, were identified. The selection criteria were, first, that the thermonuclear (TH) and beam-thermal (NB) emission components could be accurately separated using the MPR data. A limiting factor in the selection of such discharges was that the MPR had to be set to a resolution where the signal in the data is dominated by the original neutron spectrum and not the spectrometer resolution broadening. For example at 4.8% resolution the intrinsic broadening of the data is 680 keV for a neutron energy of 14 MeV. This corresponds to the broadening of the thermonuclear emission from a plasma at $T_{\mathrm{i}} = 14$ keV. At plasma temperatures much lower than this the data is dominated by the spectrometer response function, and separating the TH and NB components becomes difficult. At the 3.4% setting the intrinsic broadening is 480 keV, which corresponds to $T_{\mathrm{i}} = 7$ keV. Several discharges with $T_{\mathrm{i}} < 10$ keV had to be ruled out because the 4.8% resolution setting was used. It should be noted, though, that when only a TH component is present, such as before and after the NBI heating period, the spectrometer resolution is not a limiting factor.

Further, only discharges heated exclusively with NBI were chosen. This ensures that no other neutron emission components than thermonuclear and beam-thermal will contribute to the MPR data, besides a low energy component from scattered neutrons (see figure 3). For example if ICRF heating was used it could give rise to a high-energy supra thermal component in the MPR data, which would complicate the analysis [11]. Discharges with strong MHD activity were also avoided, since this is not accurately modeled by TRANSP/NUBEAM. Altogether this resulted in

four analyzable discharges. For the selected discharges, the time evolution of the NBI heating power, core electron density and temperature are shown in figure 2. The toroidal magnetic field and plasma current as well as the isotopic mix of the NBI and the gas puffs are given in table 2.

In figure 2 the discharges have been grouped according to the isotopic mix of the NBI. Discharges 42780, 42840 and 43011 were heated only with T beams, and the gas fueling was also almost only T (see table 2). These discharges can therefore be expected to have values of $n_{\mathrm{t}}/n_{\mathrm{d}}$ much larger than 1.0. The NBI during discharge 42647, on the other hand, consisted of both D and T. Furthermore, the main source of tritium was the beams (no T gas puffs), which means that one would expect $n_{\mathrm{t}}/n_{\mathrm{d}}$ to start at a value close to zero and then gradually increase as the NBI is turned on. It should also be noted that, in addition to the NBI and the gas injection, particle recycling at the reactor wall constitutes yet another source of fuel ions. This is discussed further in section 5.

To sum up, the selected discharges represent plasmas where fuel ion ratios from zero up to values much larger than 1.0 are expected. This makes it possible to test the $n_{\mathrm{t}}/n_{\mathrm{d}}$ measurement method for a wide range of fuel compositions.

4. RESULTS

Examples of MPR data from the selected discharges are given in figure 3 together with the fitted TH and NB components. The energy spectra of the NB components were calculated as discussed in section 2, and the TH component was modeled as a Gaussian with standard deviation and mean energy related to the plasma temperature and toroidal rotation [12]. The components were fitted to the data with their relative intensities (I_{TH}, I_{NB} and I_{Scatter}) as well as ion temperature (T_{i}) and rotational energy shift ($\mathrm{d}E$) as free parameters. For discharges 42780, 42840 and 43011 only one NB component had to be considered (NB-TD), but for discharge 42647 both NB-DT and NB-TD components had to be used since this discharge was heated with mixed beams (c.f. table 2).

In figure 4 the time evolution of the fitted values of T_{i}, I_{TH} and I_{NB} are shown for JET discharge 42840. The time resolution that can be achieved is determined by the number of events in the data as well as by the complexity of the fit. For the data acquired with the 4.8% resolution setting (see table 1) about 20 000 counts were needed in the MPR histogram to accurately fit a TH component together with a NB component. This put a neutron rate dependent limit on the time resolution. Thus, for discharge 42840 a time resolution of 250 ms could be achieved for $T\mathrm{i}$, see figure 4a. If the temperature of the TH component can be fixed the requirements on the statistics can be relaxed somewhat. In figure 4b the time resolution of I_{TH} and I_{NB} could be improved to 125 ms by interpolating T_{i} from figure 4a. For the data acquired with the 3.4% resolution setting it is sufficient with about 8 000 events in the histogram. This allowed for a time resolution of 500 ms for discharge 42780. When estimating the statistical uncertainties of the fitted parameters a non-constrained method was used; i.e., when perturbing one parameter to search for a one-sigma deviation all other parameters were allowed to vary freely and readjust to new optima. This is

important since the fitted parameters are strongly correlated, and constrained uncertainties would be a considerable underestimation of the statistical uncertainties of the fitted parameters.

In figure 5 the fuel ion ratio derived from the MPR data using the method described in section 2 is shown for the four analyzed discharges. The error-bars represent statistical uncertainty arising from the fit to the MPR data. In addition to the statistical uncertainty, the systematical error due to uncertainties in auxiliary data have also been estimated, by varying n_{e}, T_{e}, T_{i} and R_{NT} within 10% of their measured values, and recalculating the TH and NB reactivities. The corresponding changes in the estimated fuel ion ratios were added in quadrature and the resulting systematical uncertainty is represented by the dashed lines in figure 5.

For comparison, the fuel ion ratio derived from Penning trap measurements in the divertor is also shown in figure 5. It is seen that the MPR results are systematically higher than the Penning trap measurements for all cases. For discharge 42647, which was fueled with both D and T, the core $n_{\mathrm{t}}/n_{\mathrm{d}}$ derived from MPR data starts close to zero and increases to about 0.55, whereas the Penning trap does not see any significant amounts of T at any point during the discharge. All other discharges, which were fueled mainly by tritium, start with a $n_{\mathrm{t}}/n_{\mathrm{d}}$-value much larger than one and then decreases somewhat, but the MPR estimates are always higher than the corresponding Penning trap measurements.

4.1. MIXED BEAMS

As described above, two NB components are needed for the analysis of discharge 42647, since it was heated with both D and T beams. It was not possible to reliably fit the amplitudes of these two beam components independently. Instead their relative intensities were calculated from the values of n_{t} and n_{d} in an iterative process as follows.

Using a starting guess of $n_{\mathrm{t}} = n_{\mathrm{d}}$ the combined NB component, from both DT and TD reactions, is calculated using results from the TRANSP simulation. The NB component is then used in the fit to the MPR data, and the results from the fit is used to obtain a value for $n_{\mathrm{t}}/n_{\mathrm{d}}$, as described in section 2. This value is in general not the same as the starting value, and the above procedure is then repeated until the derived $n_{\mathrm{t}}/n_{\mathrm{d}}$-value is the same as the value assumed for the NB component. However, convergence is by no means guaranteed. If the initial guess is too far away from the value giving the best fit to the data, it is possible to end up in a situation where the $n_{\mathrm{t}}/n_{\mathrm{d}}$-value starts to oscillate with increasing amplitude, ultimately resulting in negative (i.e. unphysical) values. It was found that the situation could be made more stable by taking a weighted average of the ”old” and the ”new” $n_{\mathrm{t}}/n_{\mathrm{d}}$-values during each iteration, thus counteracting any tendencies of the solution to start to oscillate.

Although one more beam species complicates the analysis, it also provides an additional way of determining the fuel ion ratio. Apart from comparing the NB intensity to the TH intensity, $n_{\mathrm{t}}/n_{\mathrm{d}}$ can also be obtained by comparing the two NB components with each other (cf. equations (4) and (5)). This has been done for discharge 42647 and the results are compared in figure 6. The results

are similar for both methods; $n_\mathrm{t}/n_\mathrm{d}$ starts close to zero and gradually increases throughout the beam period. The two different estimates have overlapping error-bars for all except one time slice, i.e. they give basically the same results within the measurement uncertainties.

5. DISCUSSION

The trend of the derived $n_\mathrm{t}/n_\mathrm{d}$-values is consistent with the Penning trap measurements of the edge plasma, as seen from figure 5. That is, the higher the value of $n_\mathrm{t}/n_\mathrm{d}$ measured by the Penning trap, the higher is the corresponding value estimated by the MPR. We do however note that the estimated $n_\mathrm{t}/n_\mathrm{d}$-values from the MPR data are significantly higher than those from the Penning trap for all discharges analyzed in this paper. For discharges 42780, 42840 and 43011, this could be expected to some extent. These discharges were fueled mainly by tritium (both gas puffs and NBI), and thus the deuterium in the machine comes almost exclusively from wall recycling of residual deuterium from previous discharges. Therefore, it is not unreasonable that the Penning trap, which is located close to the carbon tiles which are the main source of deuterium, measure a higher D concentration in these discharges.

The same reasoning could possibly explain the difference in the time evolution of the $n_\mathrm{t}/n_\mathrm{d}$-values from the MPR and Penning trap measurements of these tritium fueled discharges. While the Penning trap values are approximately constant during the whole discharge the MPR results all start at $n_\mathrm{t}/n_\mathrm{d} \gg 1$ and gradually decrease and stabilize at a lower value, possibly because of the time needed for the deuterium from the walls to penetrate to the center of the plasma. In this context it is also interesting to note the difference between the MPR results for discharges 42840 and 43011, which have very similar plasma parameters, as seen from figure 2 and table 2. The time evolution of $n_\mathrm{t}/n_\mathrm{d}$ is also similar, but in 43011 it stabilizes at a higher value, $n_\mathrm{t}/n_\mathrm{d} \sim 40$ compared to $n_\mathrm{t}/n_\mathrm{d} \sim 10$ for 42840. The reason for the different fuel ion ratios in these otherwise very similar plasmas could be that there was a difference in the fueling of the discharges before them. The T/D fueling ratio accumulated over the 10 preceding discharges is 3.1 and 22, for 42840 and 43011, respectively. Hence, less deuterium has been added to the machine in the discharges prior to 43011 than 42840. One possible explanation for the different fuel ion ratios could therefore be that less deuterium is retained in the walls at the start of discharge 43011 than for 42840.

Discharge 42647 represents a different plasma scenario, where tritium entered the machine only through NBI and wall recycling. The Penning trap measured essentially no tritium at any point during this discharge. This is reasonable, given that there were no tritium gas puffs; the total T/D fueling ratio was only about 2/98. On the other hand, the NBI heating had a T/D ratio of 30/70, which was deposited mainly in the plasma core, and this tritium would be seen by the MPR but not by the Penning trap. According to the TRANSP/NUBEAM simulations of discharge 42647, the tritium deposition in the core (inside $\sqrt{\psi_\mathrm{tor}} \leq 0.3$) was about $7 \cdot 10^{18}$ m^{-3} s^{-1}. From the measurements of n_e and Z_eff it follows that the core fuel ion density, $n_\mathrm{t} + n_\mathrm{d}$, was about 2-3$\cdot 10^{19}$

m^{-3} during the NBI period (assuming only Carbon impurities). Hence, if the tritium ions can be assumed to be confined in the core for about one second after being thermalized, n_t/n_d-values of about 0.3-0.5 could be expected, which is consistent with the MPR results.

From the results in figure 5 it can be seen that the statistical uncertainty of the derived fuel ion ratios is between 10 and 20 percent. Compared to the traditionally proposed method of measuring the fuel ion ratio by comparing the thermal DD and DT emission, the method presented here is dependent on the measurement of additional plasma parameters apart from the neutron spectrum, such as the electron density and temperature, the ion temperature and the total neutron rate. This will make our results sensitive to measurement errors in these plasma parameters as well as to possible inaccuracies in the NBI slowing down modeling. The NUBEAM code itself has previously been extensively validated, both using neutron spectrometry [9] and neutron profile measurements [13], and we have, as far as possible, tried to include systematic uncertainties in our derived values of n_t/n_d with a sensitivity analysis on the most critical parameters, i.e., T_e, n_e, T_i and R_{NT}. This would, in principle, require a new TRANSP simulation for each perturbed input parameter, in order to re-evaluate equation (2) for the NB reactivity. However, here we use a simplified approach were the relative change in the reactivity is calculated from a 1-dimensional Fokker-Planck equation [14]. The original TRANSP reactivity is then rescaled accordingly.

When calculating the reactivity with TRANSP/NUBEAM the ion temperature profile is needed. In this work the profile obtained from charge exchange recombination spectroscopy (CXRS) measurements was typically used. For most of the discharges this temperature agreed well with the MPR measurement, see figure 4 for an example. The exception is discharge 42780, where the MPR estimate was up to a factor of two higher than the CXRS measurement [15]. Using the CXRS temperature for this discharge resulted in unphysical values of the total ion density, i.e. $n_d/n_e + n_t/n_e \gg 1.0$. In this case the temperature profile predicted by TRANSP was used, which was more consistent with the MPR temperature.

It would have been desirable to apply the method to pulses with fuel ion ratios closer to the optimal value of $n_t/n_d = 1.0$. Unfortunately the number of analyzable discharges was limited by the spectrometer settings used, as explained in section 3, and no suitable discharges with this fuel ion ratio could be found. However, we do expect the method presented here to work also for $n_t \sim n_d$, as long as there is sufficient NBI to separate the NB component from the TH component.

5.1. FUTURE WORK AT JET

In addition to comparing with data from the Penning trap it would be interesting to compare the results from the present method with the traditionally proposed method (comparing the thermonuclear DD and DT intensities). This would require plasma scenarios with a high deuterium fraction, so that the DD component can be distinguished from the background of scattered DT neutrons, as described in section 1 and reference [4]. We identify an interval in n_t/n_d from a few percent up to about 0.2–0.3 where the range of the two methods would overlap. JET is well suited to make these

measurements since the TOFOR [16] and MPR spectrometers provide spectroscopic capabilities for both the DD and DT emission. An excellent opportunity to make this benchmark would open up in a possible future DT campaign. This could not be done in 1997, since TOFOR was not installed at that time.

5.2. IMPLICATIONS FOR ITER

The analysis presented in this paper indicates that, in order to accurately separate the TH emission from the NB emission with high time resolution in ITER relevant plasma conditions, an energy resolution of the spectrometer of at least 3–4% is required. In this case about 10 000 counts are needed in the neutron spectrum (see section 4 and reference [17]) which means that the spectrometer must be able to operate with count rates in the order of 100 kHz if a time resolution of 100 ms is required. If the energy resolution is lower the spectrometer must be able to handle higher rates.

Furthermore, at ITER the TH emission will be even more dominating than in the discharges considered here, due to the higher plasma density. This increases the requirement on the dynamic range of the spectrometer. If the density is around 10^{20} m^{-3}, which is about 2–3 times higher than in the discharges studied here, the thermal intensity will be up to an order of magnitude higher. The NB intensity will then only be a few percent of the TH intensity, possibly even less than a percent for the optimal fuel ion ratio $n_{\mathrm{t}}/n_{\mathrm{d}} = 1$. Therefore, a neutron spectrometer is likely to need a dynamic range of three orders of magnitude in order to separate the TH and NB components in a high power ITER discharge.

6. CONCLUSIONS

It is possible to estimate the fuel ion ratio $n_{\mathrm{t}}/n_{\mathrm{d}}$ in high power DT plasmas from the ratio of the thermonuclear to beam-thermal neutron emission intensities, using a high resolution neutron spectrometer to separate the emission components. In contrast to the traditionally proposed method of measuring $n_{\mathrm{t}}/n_{\mathrm{d}}$ by comparing the thermal DD and DT peaks, the new method can estimate the fuel ion ratio for tritium concentrations from a few percent up to almost 100 percent, including the important region around $n_{\mathrm{t}}/n_{\mathrm{d}} = 1$. However, this method is more sensitive to measurement errors in other plasma parameters than the traditional method and future work should aim at comparing the two methods in plasma scenarios where both methods work.

The method has been used to estimate the fuel ion ratio in JET plasmas from the DT campaign in 1997, using the MPR neutron spectrometer. An excellent opportunity to further test this method would be in a possible future DT campaign. JET now has spectroscopic capabilities for both the DD and DT reactions, which would allow for the comparison of different ways to estimate the fuel ion ratio from neutron spectrometry data.

ACKNOWLEDGMENTS

This work was supported by EURATOM and carried out within the framework of the European Fusion Development Agreement. The views and opinions expressed herein do not necessarily reflect those of the European Commission.

REFERENCES

[1]. Korsholm S.B. et al, 2010 Review of Scientific Instruments **81** 10D323
[2]. ITER Physics Expert Group on Diagnostics and ITER Physics Basis Editors 1999 Nuclear Fusion **39** 2541–75
[3]. Kallne J, Batistoni P. and Gorini G., 1991 Review of Scientific Instruments **62** 2871–74
[4]. Ericsson G. et al, 2010 Review of Scientific Instruments **81** 10D324
[5]. Ericsson G. et al, 2001 Review of Scientific Instruments **72** 759–66
[6]. Källne J. et al, 2000 Physical Review Letters **85** 1246–1249
[7]. Pankin A. et al, 2004 Computer Physics Communications **159** 157–84
[8]. Ongena J. et al, 2012 Transactions of Fusion Science and Technology **61**(2T) 180–89
[9]. Hellesen C. et al, 2010 Plasma Physics and Controlled Fusion **52** 085013
[10]. Conroy S., 'LINE-21' Private comunication
[11]. Henriksson H. et al, 2006 Nuclear Fusion **46** 244
[12]. Brysk H., 1973 Plasma Physics **15** 611–17
[13]. Budny R.V. et al, 2000 Physics of Plasmas **7** 5038–50
[14]. Stix T., 1975 Nuclear Fusion **15** 737
[15]. Hellesen C. et al, 2012 Review of Scientific Instruments **83** 10D916
[16]. Johnson M.G. et al, 2008 Nuclear Instruments and Methods in Physics Research Section A, **591** 417–430
[17]. Hellesen C., 2010 Diagnosing Fuel Ions in Fusion Plasmas using Neutron Emission Spectroscopy Ph.D. thesis Uppsala University, Applied Nuclear Physics URL http://urn.kb.se/resolve?urn=urn:nbn:se:uu:diva-114449

JET Pulse No:	t_{foil} [mg/cm^2]	Ω_{coll} [msr]	B_{MPR} [G]	resolution [FWHM/E_n]	efficiency [10^{-6}]
42647	18	52	10288	4.8%	15.0
42780	8	40	10382	3.4%	5.2
42840	18	52	10288	4.8%	15.0
43011	18	52	10288	4.8%	15.0

Table 1: Settings of the MPR spectrometer that were used in this paper.

JET Pulse No:	B_T [T]	I_p [MA]	NBI [n_t/n_d]	Gas [n_t/n_d]
42647	3.45	3.4	30/70	/100
42780	3.0	2.9	100/	97/3
42840	3.45	3.8	100/	93/7
43011	3.45	3.8	100/	91/9

Table 2: Global plasma parameters in the discharges studied.

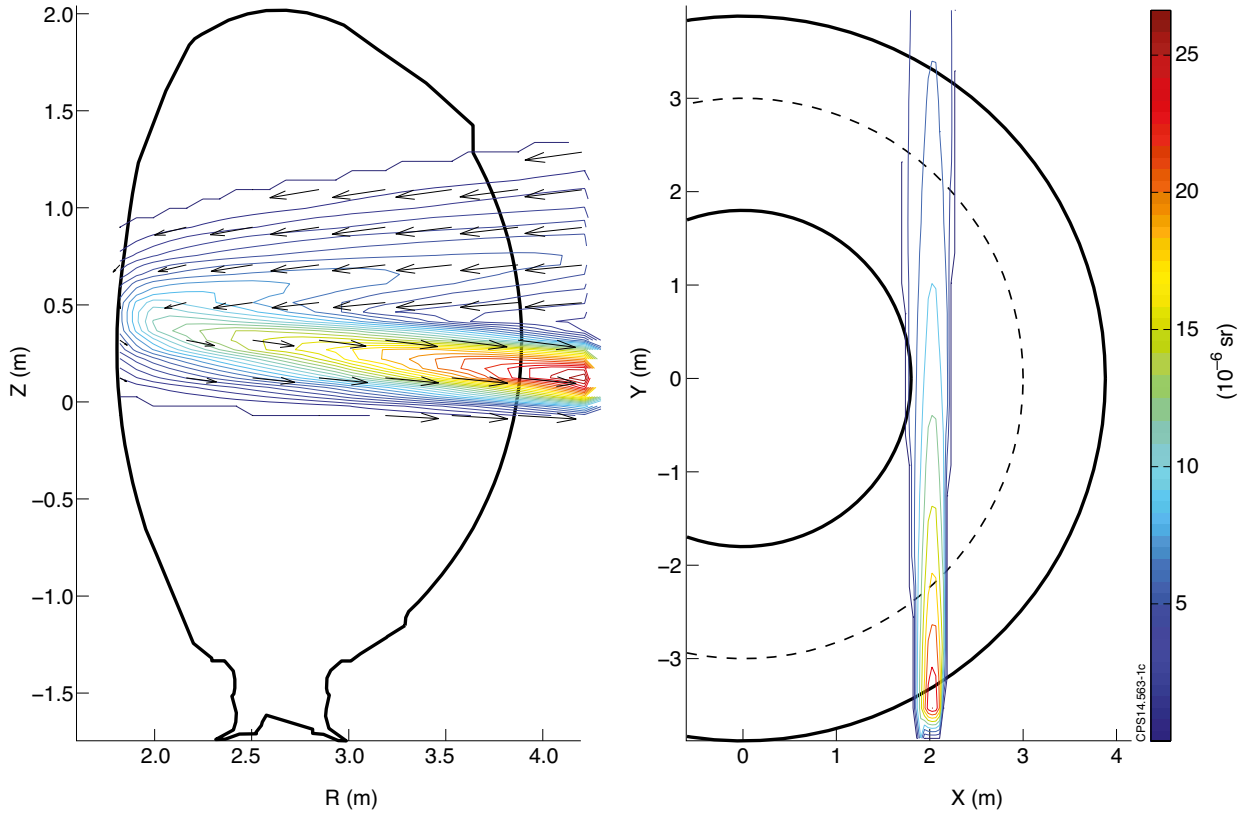

Figure 1: Illustration of the MPR sight line showing the position dependent solid angle projected on the RZ (left) and XY (right) planes. In the RZ projection the direction $\boldsymbol{u}$ *towards the spectrometer is also shown. The spectrometer is located at position x = 2.07m, y = −9.88m, z = −0.37m. The outline of the JET first wall is shown as solid black lines and the magnetic axis as a dashed line.*

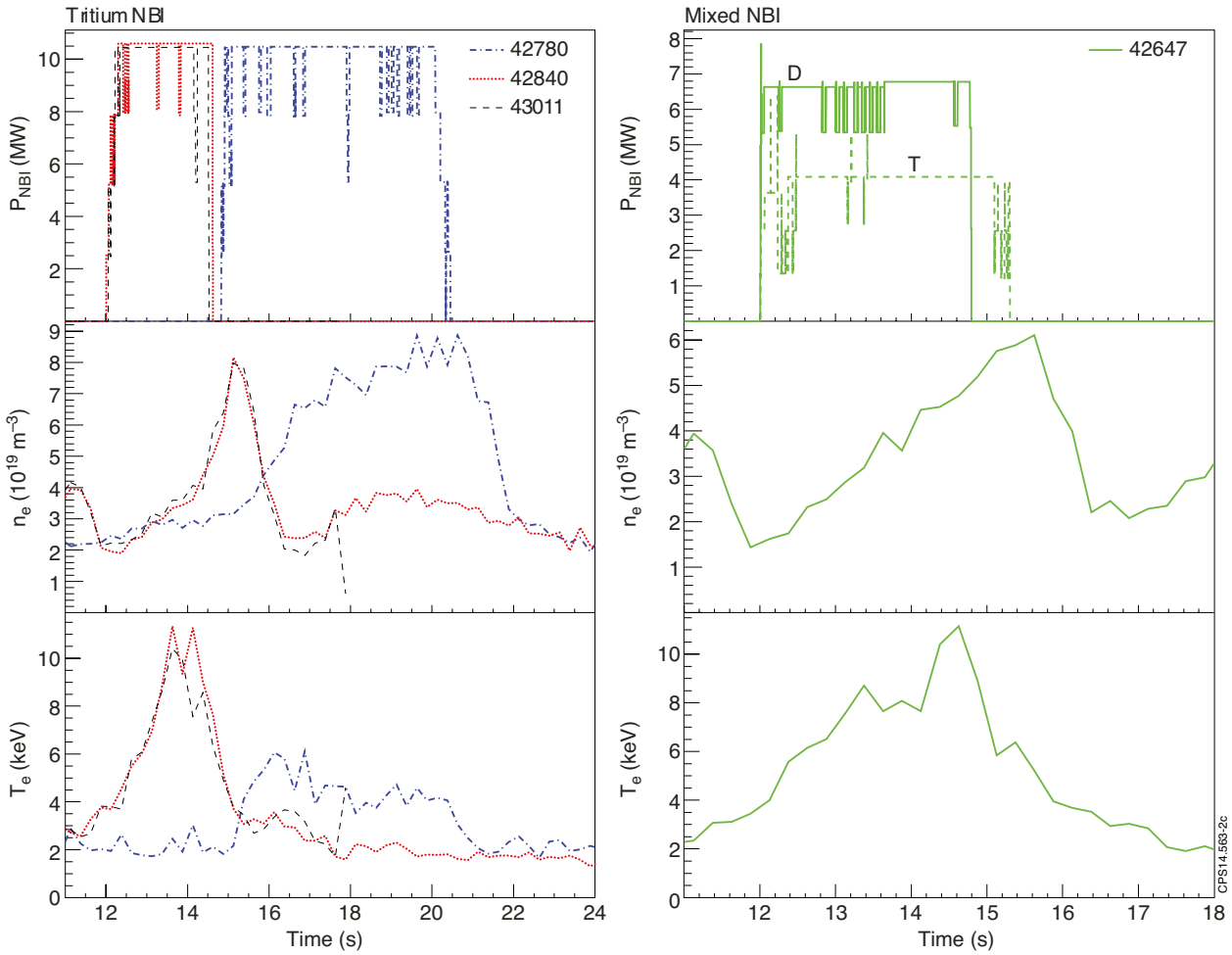

Figure 2: Neutral beam power, core electron density and core electron temperature for the four JET Pulse No's studied. The discharges are grouped according to the isotopic mix of the NBI (see table 2); the left panel shows the discharges with pure T beams and the right panel shows the discharge with mixed (both D and T) beams.

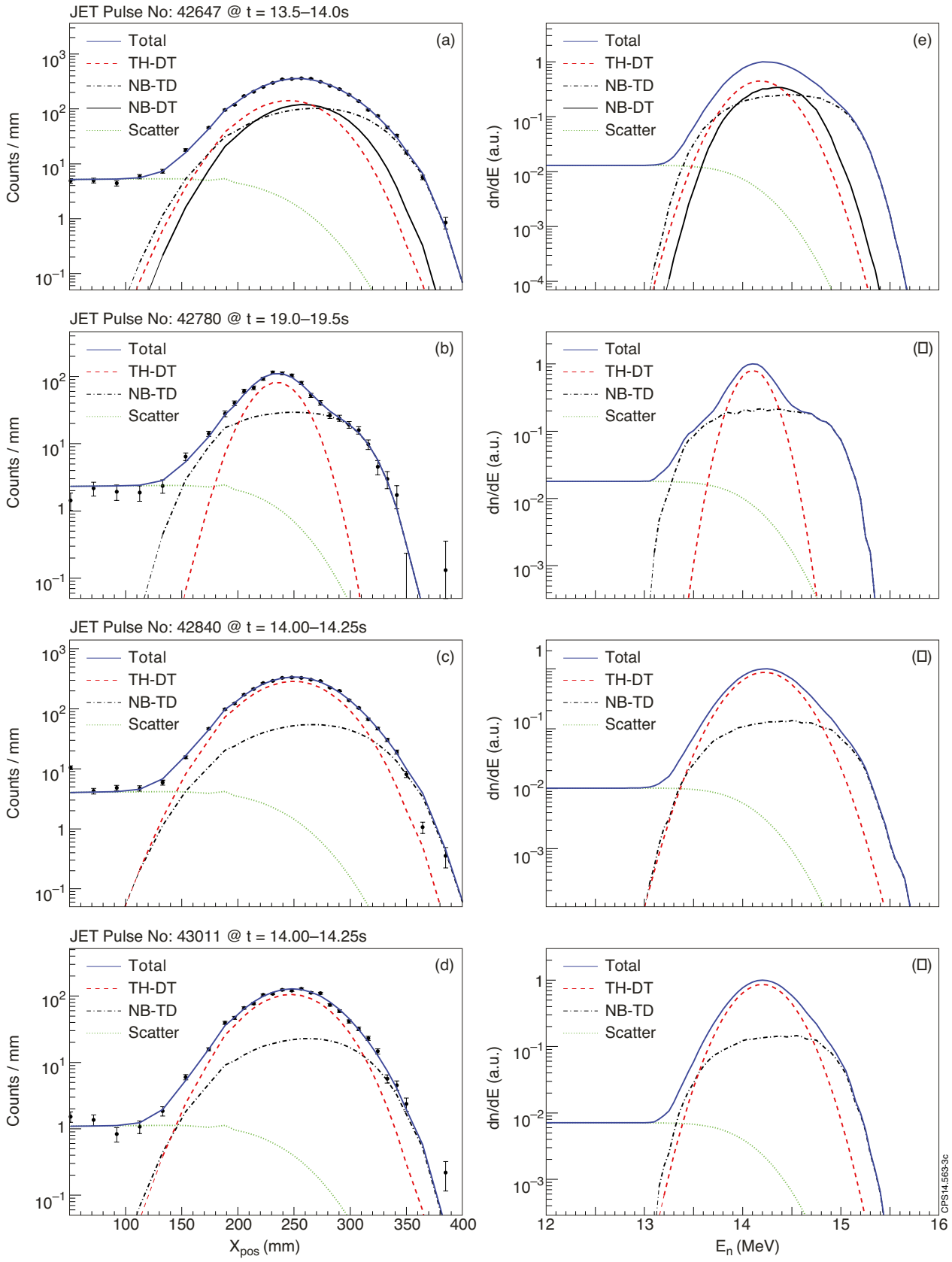

Figure 3: Examples of MPR data with fitted TH, NB and Scatter components for Pulse No's: 42647, 42780, 42840 and 43011 in (a), (b), (c) and (d), respectively. The energy representation of the components are shown in (e), (f), (g) and (h).

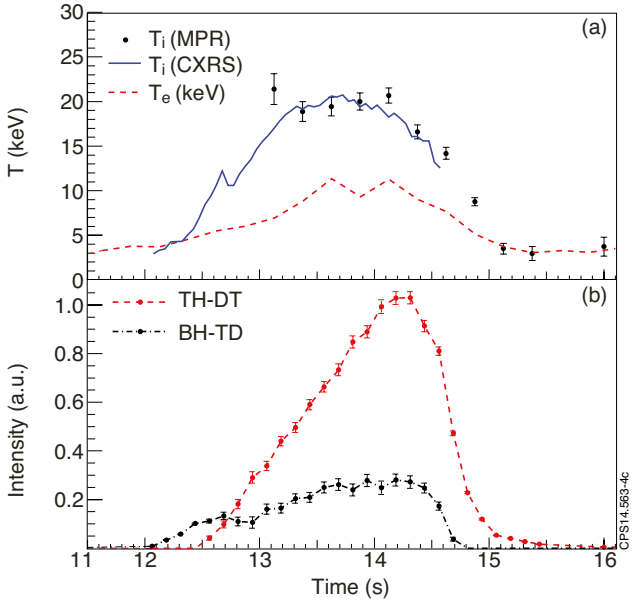

Figure 4: Time evolution of the fitted on-axis temperature (a) and component intensities (b) for JET Pulse No's: 42840. For comparison the central ion and electron temperatures measured by charge exchange (CXRS) and Thomson scattering (TS) diagnostics are also shown in (a).

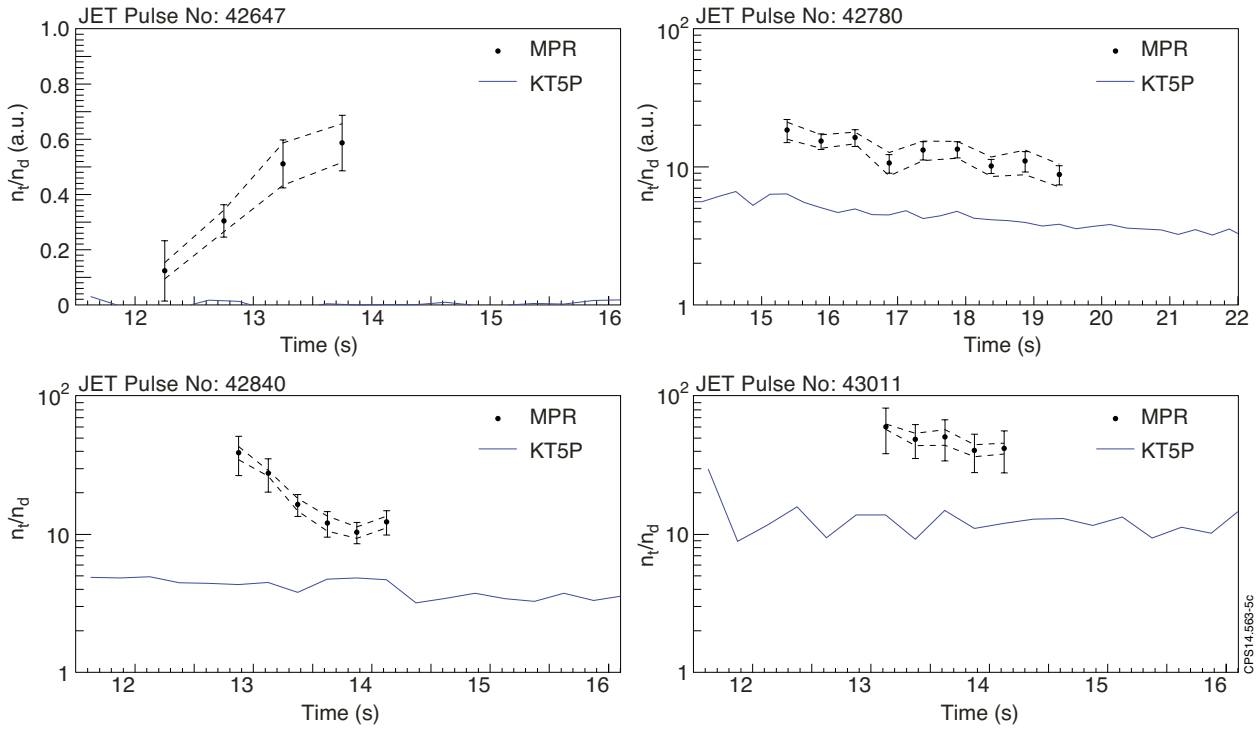

Figure 5: Derived fuel ion ratios for the four analyzed discharges (points with error-bars). The dashed lines represent the systematical uncertainty due to uncertainties in auxiliary data. For comparison, the fuel ion ratio measured in the divertor by the Penning trap (KT5P) is shown in solid blue.

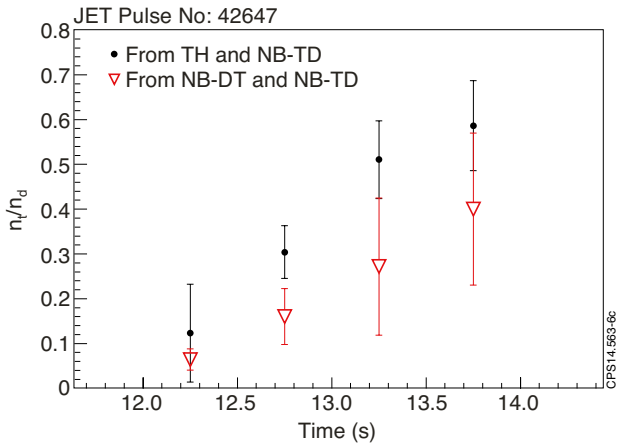

Figure 6: Fuel ion ratios for Pulse No: 42647 estimated in two ways; from the TH and NB-TD components (blue crosses) and from the NB-DT and NB-TD components (red triangles).